JO JOURNAL OF OSSEOINTEGRATION periodontics and prosthodontics

# Histological and histomorphometrical evaluation of porous phosphate glass as a bone graft substitute: A pilot study

A. CHAUDHARI[1], N. CHAUHAN[1], S. ANOOP[2], S. PATIL[2], R. V. CHANDRA[3], N. LAKHKAR[1]

[1]SynThera Biomedical Pvt. Ltd., India
[2]Palamur Biosciences Pvt. Ltd., India
[3]SVS Institute of Dental Sciences, India

TO CITE THIS ARTICLE
Chaudhari A, Chauhan N, Anoop S, Patil S, Chandra RV, Lakhkar N. Histological and histomorphometrical evaluation of porous phosphate glass as a bone graft substitute: A pilot study. J Osseointegr 2022;14(2):88-96.

DOI 10.23805/JO.2022.14.17

## ABSTRACT

**Aim** To overcome the disadvantages of auto-, allo-, and/or xenografts (XG), porous synthetic bone graft substitutes are considered as suitable alternatives. The aim of this animal study was to determine the bone regeneration potential of a synthetic bioactive porous phosphate glass (PPG) in comparison with a commercially available XG.

**Materials and methods** Defects were created by making 4 mm holes in each rabbit femur and in a cavity of approximately 5 X 8 X 40 (W X D X L) $mm^3$ made in Beagle dog mandibles after removing the incisors. Empty cavities were used as negative controls in both the evaluation models. Cavities thus made were grafted with the bone grafts (PPG or XG) or kept empty. Histological and histomorphometrical analyses were carried out post-ex-plantation at specific time points.

**Results** Histologically, partial to almost-complete degradation of the grafts was observed in the rabbit femur and Beagle dog mandible models. Bone regeneration was observed within the bulk of the PPG but not in XG particles. Bone regeneration by PPG and XG was histomorphometrically analyzed in Beagle dog mandible model. A higher standard deviation was observed for XG compared to PPG in histomorphometrical analyses at all the healing points.

**Conclusion** The results indicate that PPG is a bone graft that promotes osteoconductivity and bone regeneration when compared to a commercial XG but with better predictability.

KEYWORDS Porous bioactive glass; Bone regeneration; Biodegradable bone graft.

## INTRODUCTION

Use of bone grafts is a common practice for the treatment of skeletal defects resulting from trauma, disease, surgery and congenital conditions. Bone grafts are supposed to be degraded completely and replaced by the host-like bone through osteogenesis and remodeling. Autograft is considered the gold standard due to its osteoconductive, osteoinductive and osteogenic properties (1). However, it is well known that autograft usage is associated with major disadvantages such as donor site morbidity (2, 3) and other possible issues such as hematoma formation, nerve injury, blood loss, unaesthetic defects etc. with an added expense incurred due to additional surgical procedures. Also, there is always a limit to the volume of bone that can be harvested from each donor site. Therefore, for grafting procedures requiring larger amounts of graft materials, allografts or xenografts are preferred. Although both allo- and xeno-grafts have reduced osteoinductive properties due to processing required for biocompatibility, and sterilization (4), they have a distinctive advantage of easy availability and surgical protocol over autografts. However, they carry an uncommon risk of an immune reaction, and their inability to regenerate bone in large defects.

To avoid the disadvantages of biologically sourced bone grafts (auto-, allo-, and xeno-grafts), synthetic bone grafts (alloplasts) can be used for the treatment of bone defects (5). They are readily available sterile products, but they lack in osteoinductive properties if not used in combination with biologically sourced additives (6). One of the most important properties required of synthetic bone graft substitutes is their porous nature and their complete biodegradation (7). It is advantageous to have the biodegradation products supporting the process of bone regeneration at a rate similar to the new bone formation. Bioactive glass-based bone graft substitutes can have all these properties (8-10). Silica based Bioglass products are commercially available since the last few decades. Their degradation products support bone regeneration by up-regulating the expression of genes (8) especially IGF-II along with IGF binding proteins and



 

proteases that cleave IGF-II from their binding proteins (11). But it is difficult to process these materials to form porous structures that can provide the scaffolding effect during the healing of host tissue after the grafting procedure and at the same time retain the bioactivity of the original bioactive glass material (12).

Phosphate bioactive glass materials are suitable candidates for bone regeneration applications (9, 10). The advantages of phosphate glass are their linear degradation in aqueous environment (13) and no presence of silica, an element which is not native to natural bone tissue. Also, it is possible to change the ion release profiles by simply changing the composition of the glasses (14, 15). Production of glasses is generally achieved by melt quenching process as it is an easy, reproducible and scalable process. Gel casting is a suitable method for production of porous glass scaffolds of glasses made by melt quench method (16). It is a method by which porous foam is formed by stabilizing air bubbles (created by surfactant) in a gel of polymer and the glass particles (17). With this method, a porous bone graft substitute material was made from a bioactive titanium phosphate glass (hereinafter referred to as PPG for porous phosphate glass). It has already been reported that the titanium phosphate glass is suitable for bone regeneration (18). The effect of imparting porosity to such glass on bone regeneration needs to be evaluated. In this context, the bone regeneration potential of PPG was evaluated in two different animal models viz. rabbit femur and Beagle dog mandible in a pilot study. Data was obtained from histological and histomorphometrical analyses to understand the bone regeneration performance of the material.

## MATERIALS AND METHODS

### PPG production

PPG was produced according to the procedure described by Chauhan et al. (17). The glass required for PPG production was made with a composition (in mol %) of 50% $P_2O_5$, 40% CaO, 5% $Na_2O$ and 5% of $TiO_2$. Pre-calculated amounts of $CaCO_3$ (99%, Finar, Ahmedabad, India), $Na_2CO_3$ (99%, Merck, Darmstadt, Germany), $TiO_2$ (99%, Sigma, Saint Louis, MO, USA) and $P_2O_5$ (98%, Loba, Mumbai, India) were mixed and then melted at 1300˚C for 1 h in a Platinum/10% Rhodium crucible using a raising hearth furnace (Ants Ceramics, Mumbai, India). After the melting, the glasses were quenched by pouring on to a steel plate at room temperature. The glass obtained using the above procedure was excessively ground using a planetary mini ball mill (Insmart, Hyderabad, India). Appropriate quantities of glass particles, distilled water, methacrylamide (TCI, Tokyo, Japan), N N' methylene bisacrylamide (Loba, Pune, India), ammonium polyacrylate (Commercial name: Dispex, Kindly gifted by BASF, Mumbai, India), and Triton X100 (Loba, Mumbai, India) were mixed using the overhead mechanical stirrer (Ika, Staufen, Germany). A foamy liquid was formed to which ammonium persulfate (Loba, Mumbai, India), and tetramethylene diamine (Loba, Mumbai, India) were added and stirred thoroughly before gelling. The sintering of the foam was carried out at 625°C for 1 h. The blocks were then crushed and sieved to achieve particle fraction between 420 µm (BSS 36) and 850 µm (BSS 18) mesh.

### Surface characterization of PPG by Scanning Electron Microscopy (SEM)

PPG granules were mounted onto carbon adhesive discs attached to aluminum SEM specimen stubs. The assembly was then sputter-coated with gold by Polaron E5100 (Polaron, Milton Keynes, UK). The coated samples were observed with a scanning electron microscope (model JSM 5410LV, JEOL, Japan) using various magnifications at an operating voltage of 20 kV. Images were taken at magnifications of 100X, 500X, 2000X and 3000X.

### Surgery

Participants and interventions: All animal experiments were carried out according to the ARRIVE guidelines at Palamur Biosciences Pvt. Ltd. The study was conducted in New Zealand white rabbits (11 animals; randomly chosen gender; mean weight = 2.09 kg) and Beagle dogs (8 animals; randomly chosen gender; mean weight = 9-14 kg) which were in-house bred at Palamur Biosciences. The animals were maintained in environmental conditions as prescribed by the ARRIVE guidelines. Institutional and national guidelines were followed for the care and use of the animals in this study. All protocols related to experiments on rabbits were approved by the Institutional Animal Ethics Committee of Palamur Biosciences (PAL/IAEC/2017/12/02/84). Furthermore, all protocols related to experiments on Beagle dogs were approved by the Committee for the Purpose of Control and Supervision of Experiments on Animals (CPCSEA), which were earlier recommended by the institutional animal ethics committee of Palamur Biosciences (PAL/IAEC/2018/04/01/06).

Test and control groups: PPG was the test group and a commercially available XG (Bio-Oss, Geistlich Pharma, Switzerland) was used as a positive control group. Both materials were supplied to Palamur Biosciences in sterile condition (PPG sterilized by ethylene oxide and XG as received) for evaluation for efficacy in rabbit femur and Beagle dog mandible models. In both models, empty cavities without bone grafts were the negative controls.

Rabbit femur model: Medial side of both femora of New Zealand white rabbits (Palamur Biosciences, Mahabubnagar, India) was clipped free of fur. Intramuscular injections of 4 mg/kg of xylazine followed by 3 mg/kg of ketamine were administered to each animal. Each rabbit was then injected subcutaneously with 0.02 mg/kg buprenorphine. The surgical site was scrubbed with a germicidal soap, wiped with 70% isopropyl alcohol, and painted with povidone iodine. One single incision was

made to open the site for the surgery. Skin incision was followed by the removal of fasciae and muscles. The bone surface was exposed. A hole of 4 mm diameter was drilled using a trephine burr. The drilling was carried out at low speed and under continuous irrigation with physiological saline solution. Only one defect was made on each femur. The positions of all the defects were such that the cavity always had direct access to the bone marrow. The bone grafts (PPG and XG) were mixed with saline solution to make a paste for easier handling. Each cavity was randomly filled with the pastes of the bone grafts (4 animals for each time point). In one animal at each time point, two holes were made, one in each femur and kept as negative controls without any graft to understand the effect of the surgical procedure. Each wound was then closed by using suitable sutures. After the surgery, all animals received subcutaneous analgesia (Carprofen 10 mg/kg) for 3 days starting from the day of the surgery and povidone iodine was applied over the wound. During the healing period, all the animals were allowed unrestricted mobility. A rabbit from the 6 week healing period group fractured its leg after 4 days of surgery. Therefore, this animal was not considered for further investigation and the surgery was repeated on another animal. Half of the animals (4 animals with bone graft implantations and 1 animal with 2 negative controls in each femur) were sacrificed after 2 weeks and the remaining animals (4 nos.) after 6 weeks. The femora of both legs of the sacrificed animals were removed and all the soft tissue on the bone was removed without damaging the implantation site. These samples were blind-labeled and stored in 10% buffered formalin solution for cell and tissue fixation until further processing for tissue analyses. One animal (apart from the 10 animals) was implanted with PPG (in one femur) for analysis using micro-computed tomography (micro-CT). This animal was sacrificed after 2 weeks and the sample was recovered and stored in formalin solution until analysis.

Beagle dog mandible model: All surgical interventions on the Beagle dogs were performed under general anesthesia in aseptic conditions. All animals were subjected to sedation using intramuscular injection of xylazine at a dose rate of 1 mg/kg, after administration of pre-anesthetics, induction of anesthesia was performed by intravenous administration of propofol at a dose rate of 3 mg/kg and later anesthesia was maintained with propofol at the infusion rate of 0.6 mg/kg/min. In addition, regional anesthesia was provided by injecting the anesthetic solution of lidocaine 2% (1 mg/kg). Pre-emptive analgesia was given using meloxicam subcutaneously (0.2 mg/kg) and later it was followed by post-operative analgesia using meloxicam at the rate of 0.1 mg/kg. During the operation, animals were observed for the pain and other complications. At the baseline, all lower anterior teeth (excluding the canines) were carefully removed. After ensuring that the roots were removed, bone defects were created to approximate dimensions of 5 X 8 X 40 $mm^3$ (Width X Depth X Length). The cavity was virtually divided in to 2 quadrants for the ease of surgeons to place 2 bone grafts or one bone graft and an empty cavity. The defects (total 16) were either filled with the bone grafts (PPG or XG) or kept empty as negative controls. Before filling into the defect, the bone grafts were mixed with saline and carefully placed to fill the bone defect. In both quadrants, the flaps were adjusted to allow full coverage of the edentulous ridge and sutured. A 6-month period of plaque control, consisting of daily cleaning of the operated area was initiated. At the end of this period, a clinical examination including assessment of plaque and soft tissue inflammation was performed. All the 8 animals were euthanized at this point (6 months). The mandibles were removed and placed in a fixative solution ($CaCO_3$ buffered formalin solution).

## Micro-CT evaluation of PPG implanted in rabbit femur

The tissue sample recovered for micro-CT analysis was evaluated using Scanner type 10 desktop Micro-CT equipment (µCT-40, Scanco Medical, Basseldorf, Switzerland). The tissue sample was scanned at 12 µm voxel resolution with an integration time of 300 ms, at 45 keV with 177 µA current. Two dimensional images were taken in cross-sectional and transverse directions.

## Histological and histomorphometrical analyses

Preparation of slides for microscopy: The tissue samples of rabbit femora and Beagle dog mandibles stored in formalin were de-calcified in acetic acid and nitric acid respectively and cut into smallest possible size without damaging the bone graft implantation site. The de-calcified bone tissue samples of the rabbit femora and Beagle dog mandibles were dehydrated in increasing concentration of alcohol. The sections were then embedded in paraffin wax. The embedded tissue samples in paraffin wax were sectioned at right position using a microtome so that the cross-sectional view of bone-graft-implantation site is clearly visible. These sections were then transferred to glass slides and stained with Hematoxylin and Eosin (HE). The sections were observed under light microscope and images were taken using 10X objective. As one image was not enough to visualize the complete section, many images of the same section were taken so that complete section could be mapped in a serpentine panorama fashion and then stitched together to get a single image of the complete section by Image Composite Editor (Microsoft Corporation; Version 2.0.3.0). The images shown in Figures 1a and 2a are typical examples of HE stained histological sections of Rabbit femora and Beagle dog mandibles.

Histomorphometrical analyses: Histomorphometrical analyses were carried out using FIJI (19) with an installed plugin called BoneJ (20). The bone regeneration area (BRA) (Fig. 2b) is the area where the bone graft was implanted. For histomorphometrical analysis of Beagle dog mandible model, the BRA (Fig. 2c) was analysed by

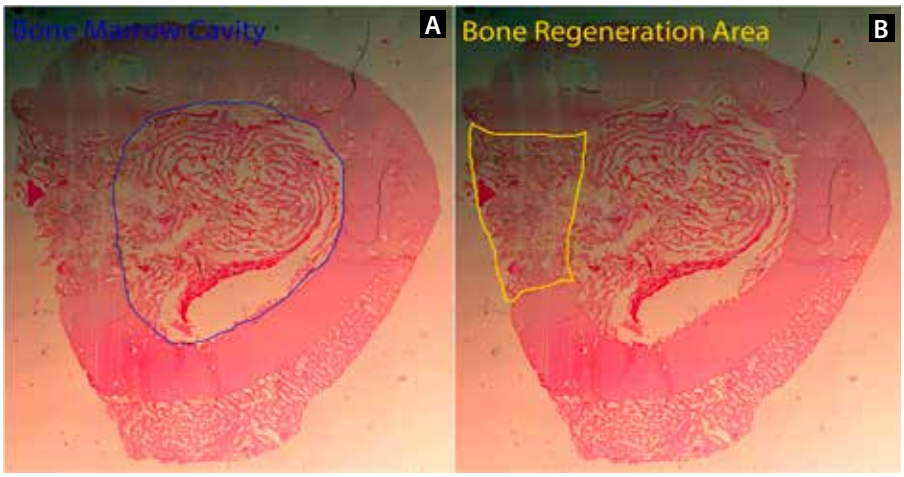


FIG. 1 HE stained tissue section (representative) for evaluation of effect of bone graft on bone regeneration in New Zealand white rabbit femur: A typical section taken perpendicular to the longitudinal axis of bone (a); The regions used for histological evaluation of regenerated bone in BRA (marked by yellow line) (b).

separating it from rest of the image. This image was then converted to a binary image by first converting it in to 8-bit image and then the threshold of the image is adjusted by comparing it with the original image of the section for bone recognition. After running the BoneJ plugin ("Area/Volume Fraction" script), the area ratio of bone area (BA) in BRA and total area (TA) of BRA ($BA_{BRA}/TA_{BRA}$) was obtained. Similarly, area ratio of BA in control area (CA) and TA of CA in the host bone tissue region ($BA_{CA}/TA_{CA}$) was determined. This BA ratio of the CA was used to normalize the effect of the original host bone tissue. Bone area fraction (BAF) was calculated using the following formula.

$$\left[\left(\frac{BA_{BRA}}{TA_{BRA}}\right)\Big/\left(\frac{BA_{CA}}{TA_{CA}}\right)\right] \times 100 = BAF\ [\%]$$

$BA_{BRA}$ = Bone area (BA) in the Bone Regeneration Area (BRA)
$TA_{BRA}$ = Total Area (TA) of Bone Regeneration Area (BRA)
$BA_{CA}$ = Bone Area (BA) of control Area (CA)
$TA_{CA}$ = Total Area (TA) of Control Area (CA)
$BAF$ = Bone Area Fraction (a fraction of BRA occupied by regenerated bone)

## Statistical analyses

For comparison between test and controls, the BAF determined after histomorphometrical analysis is represented as Mean ± Standard Deviation (SD). Statistical analyses were performed using Microsoft Excel (Microsoft Corporation; Microsoft Office Standard 2010) via the ANOVA: Single factor. A 95% confidence level was considered significant. The differences are indicated in the graphical representations, if any.

# RESULTS

## Surface characterization of PPG by SEM

SEM images are shown in Figure 3 (Magnifications: 100 X, a; 500 X, b; 2000 X, c; 3000 X, d). The surface of PPG granules is characterized by open holes with size in the range of 100-300 µm (Fig. 3a). The surface also has smaller holes in the range of 10 to 50 µm (Fig. 3b-3d). The surface is very porous in nature and suitable for cell proliferation. The smaller pores indicate an open and interconnected internal structure.

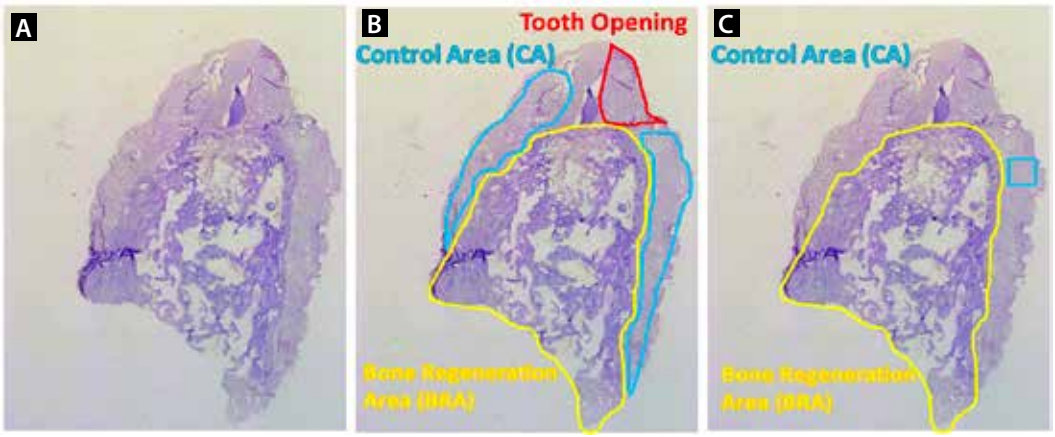


FIG. 2 HE stained tissue section (representative) for evaluation of effect of bone graft on bone regeneration in Beagle dog mandible. (This particular section is of PPG implanted in Beagle dog mandible.) A typical mesio-distal section (a); The regions used for histomorphometrical evaluation of regenerated bone in BRA (marked by yellow line) normalized by evaluation of bone present in the host tissue CA (marked by a blue line) (b); The actual BRA and CA used for the evaluation of histomorphometrical parameters (c).

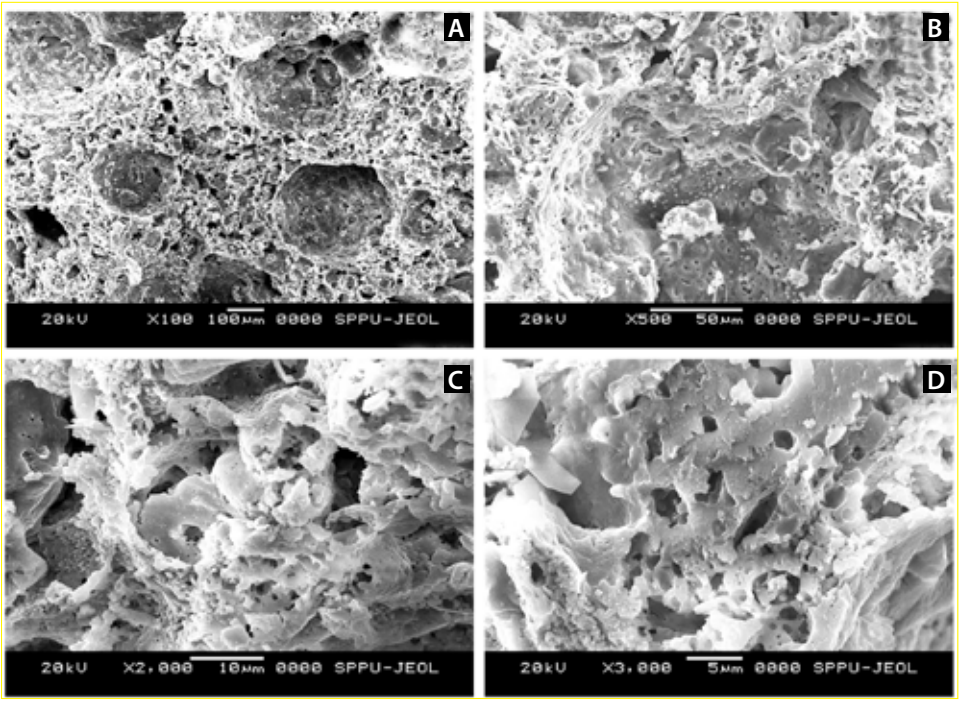


FIG. 3 Scanning Electron Micrographs of PPG surface: The images were taken at increasing magnifications of (a) 100X (Scale bar=100 µm); (b) 500X (Scale bar=50 µm); (c) 2000X (Scale bar=10 µm); and (d) 3000X (Scale bar=5 µm).

## Micro-CT evaluation of PPG implanted in rabbit femur

Figure 4a and 4b are 3D images of the bone taken at the graft site by micro-CT. Yellow arrows indicate the hole made in the bone during the surgery to study bone regeneration as an effect of the graft. During the surgery, PPG was grafted in this hole which is open to the bone marrow cavity as well as the muscle and skin. The red arrows indicate the tissue reaction to the bone graft material inside the bone marrow cavity. No adverse reaction by the host tissue to the bone graft was observed. To visualize the presence of PPG, images were also taken in 2D to show implantation site in the cross-sectional and transverse direction (Fig. 4c and 4d respectively). The blue arrows indicate PPG particles. It is observed that PPG particles are present in the hole after 2 weeks of implantation. From the 2D images, commencement of the bone regeneration process from the edges of the host bone tissue is clearly observed.

## Histology

In the rabbit femur model, the control samples (empty cavities) could not be identified possibly due to filling with soft tissue and blood clot. In general for both the evaluation models (Fig. 1, 2), no inflammatory reaction was observed for the evaluation periods. In the BRA, lamellar bone, bone marrow and traces of woven bone could be observed. In the Beagle dog mandible model, the appearance of woven bone is more than that for the rabbit femur model. But this information needs a caution due to differences in the healing periods and animal models. In all the sections for both the models, bone remodeling was observed where host bone was in contact with the bone grafts typically in the BRA (represented by yellow boundary). For rabbit femur model, more bone regeneration in the BRA was observed histologically after 6-week healing period as compared to the healing period of 2 weeks.

The resorption of the bone graft particles during the healing period was observed in both the evaluation models. In the rabbit femora sections where PPG was grafted, porous PPG granules were seen degrading when the healing periods of 2 weeks and 6 weeks (Fig, 5a, 5c indicated by yellow arrows) were compared. Similarly, the degradation of XG was not complete after 6 weeks of healing (Fig. 5b, 5d indicated by purple arrows). After the healing period of 2 weeks, the XG particles are mostly intact. On the contrary, the XG particles seem to be degraded but still present after the healing period of 6 weeks. The degradation could be observed due to the gap observed between the XG particles and the surrounding tissue. It could be observed that at both healing periods, the bone regeneration and remodeling process has started within the bulk of the PPG particles. In the Beagle dog mandible model, the degradation of bone graft particles was compared after 6 months of healing period. The representative images for PPG and XG are respectively shown in Figure 6a and 6b. The graft particles or their locations are indicated by the yellow and the purple arrows for PPG and XG sections respectively. In general, the PPG particles are very rarely observed. In the 2-D images of the sections, the bone regeneration in the porous structure of PPG particles could be observed. The regenerated mature bone could be observed in the pores of the particles. On the other hand the XG particles were not observed at all. Only their cavities after their complete degradation could be observed.

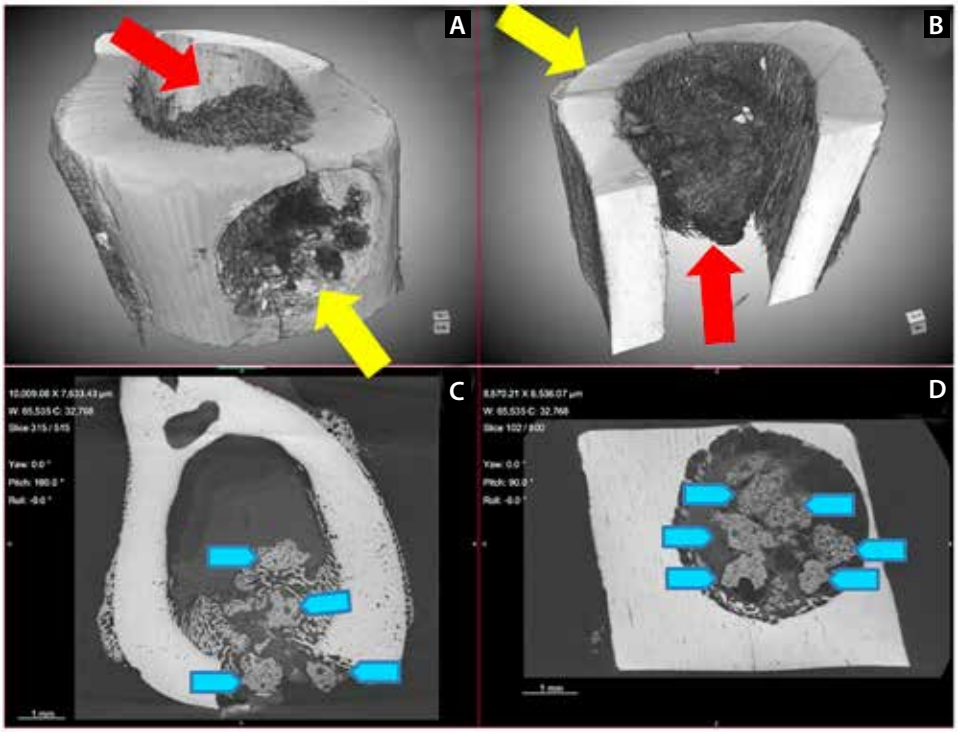


FIG. 4 Micro-CT images of the bone with grafted PPG: (a) 3-D view focusing on the outer surface of bone. The yellow arrows indicate the hole made in the bone; (b) 3-D view focusing on the inner side of the bone (or bone marrow) and the red arrows indicate the tissue reaction to the grafting procedure after 2 weeks of healing; (c) 2-D image in cross-sectional direction (parallel to drill axis); (d) 2-D image in transverse direction (perpendicular to drill axis) and the blue arrows indicate PPG particles (Scale bar=1 mm).

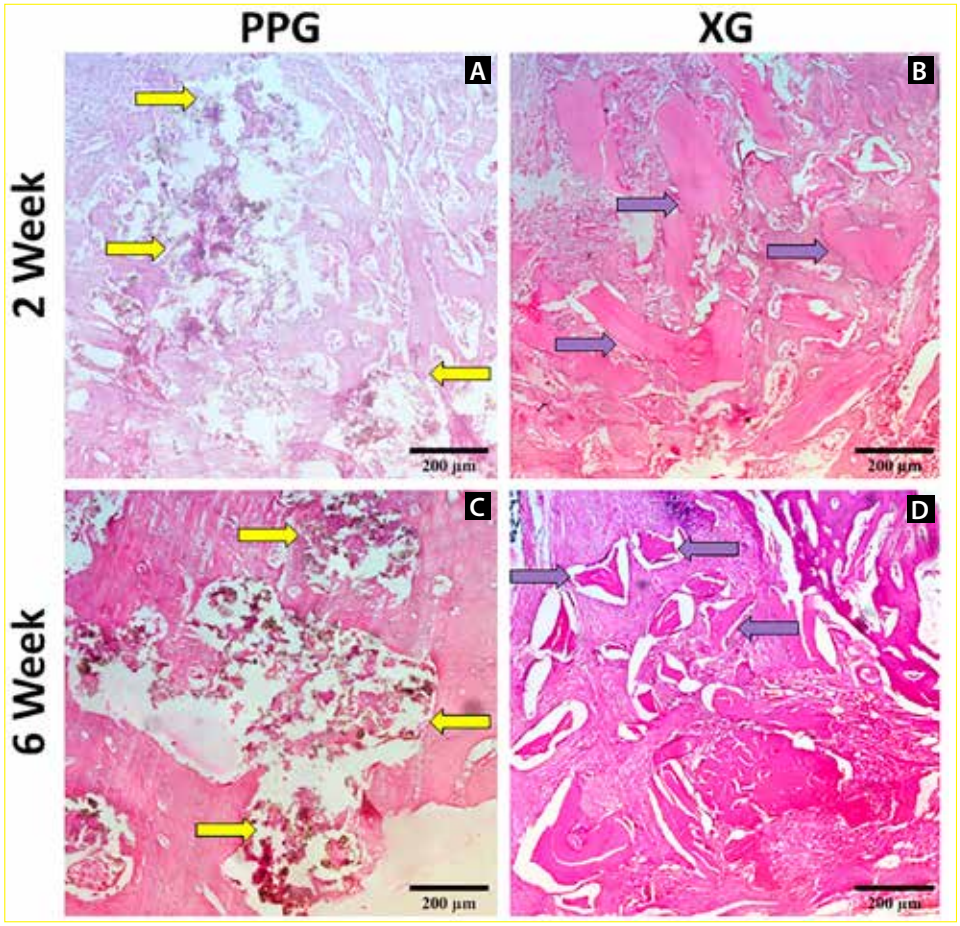


FIG. 5 Histology evaluation of rabbit femora as an effect of bone grafting: Typical examples of histological sections of (a) PPG after 2 week healing; (b) XG after 2 week healing; (c) PPG after 6 week healing; and (d) XG after 6 week healing period.

## Histomorphometry

As mentioned above, the control samples for rabbit femur model could not be identified and therefore histomorphometry was not conducted for this model. The histomorphometry results for the Beagle dog mandible model are shown in Figure 7. After 6 months

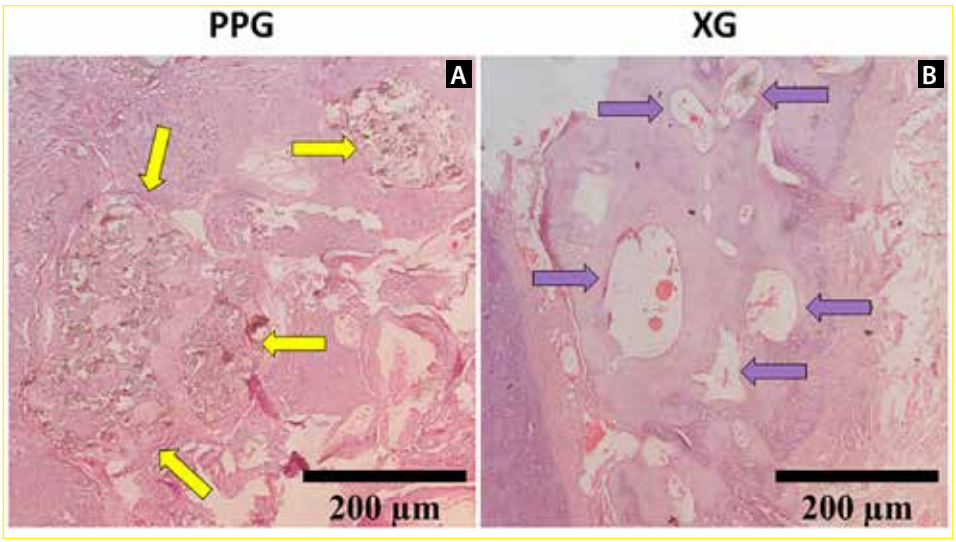


FIG. 6 Histology evaluation of Beagle dog mandible as an effect of bone grafting: Typical examples of histological sections of (a) PPG; and (b) XG after 6 month healing period.

of healing, the difference between the BRA measured for the controls (67.96±14.24), XG (74.14±9.71), and PPG (70.76±4.90) was statistically insignificant ($p>0.05$). This indicates that the amount of bone regenerated as an effect of bone graft implantation is similar. Moreover, it can be observed that the standard deviation in case of PPG is smaller than XG.

## DISCUSSION

Implantable biomaterials interact with the surrounding tissue via the material surface. This phenomenon is more important in the case of bone graft substitutes because of the requirement of porous tissue regeneration. The graft substitute needs to be porous in such a way that its porous structure is similar to that of the host bone tissue (21). Such structure of the graft is required because it is expected of the graft to get resorbed while simultaneously regenerating a porous bone tissue. The components of resorption should support bone regeneration which ideally should be at the same rate as graft resorption (22). Thus, from a materials point of view, a bone graft substitute should have the porous structure similar to the bone; the resorption components should support bone regeneration; and the graft's resorption rate should be the same as the rate of new bone tissue formation.

In this pilot study, the bone regeneration potential of PPG was evaluated *in vivo* in rabbit femur and Beagle dog mandible models. PPG is a porous bone graft substitute with a possibility of varying the composition and porous structure as per the surgical requirements (17). The open and interconnected porous structure of PPG as observed in the SEM images (Fig. 3) shows that the internal surface is accessible to the biological environment after grafting. The internal pore structure is formed due to overlapping of the air bubbles during the process of gel formation (17). Such interconnected pore structure is useful during the bone regeneration and the healing process in general by providing mass transport required for the process. Also, due to the presence of internal volume and surface for cell proliferation, the eventual vascularization of the bone can be easily realized (23, 24).

The rabbit femur model study was designed to evaluate the effect of biomaterials in the vicinity of host bone on bone regeneration in a smaller animal. There are many studies which have used the rabbit tibiae or femora for such evaluations (25-28). A major advantage is the continuous supply of blood and other nutrients required for healing and bone regeneration which is usually the case for treatment involving bone graft materials. On the other hand, the disadvantage is the difficulty of ensuring that a particulate bone graft remains in place throughout the healing period. Indeed, the graft is unlikely to remain in place as observed from the results of micro-CT (Fig. 4c).

It is clear from these results that the bone graft can move only into the bone marrow cavity and does not move towards the outer bone surface. Although the graft

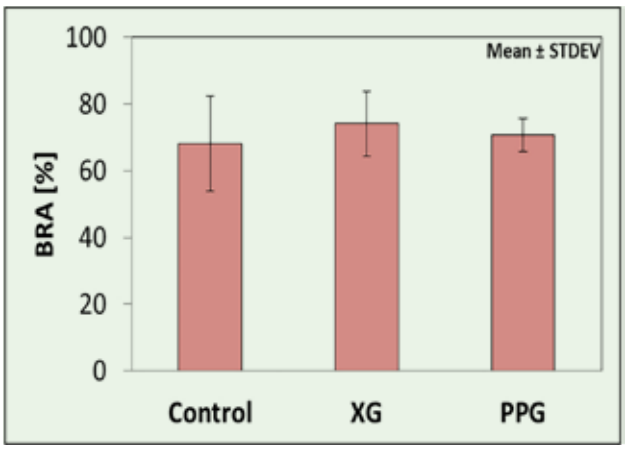


FIG. 7 Histomorphometrical evaluation of bone grafts in Beagle dog mandible model: Bone Area Fraction (BAF) comparison of PPG (N=6) with XG (N=5) and Control (N=5) for 6 month healing period. The results are Mean ± STDEV. No significant differences were observed ($p>0.05$).

does not remain in place entirely during the course of the healing period, the histological analysis of rabbit model samples (Fig. 1, 4, 5a, 5c) show bone regeneration in the cavity made in the cortical bone. Also, as mentioned in the results, the negative controls could not be identified. To avoid the above mentioned disadvantages of the rabbit femur model, a bone graft study was carried out in Beagle dog mandible model. In this study, the bone grafts were confined to a cavity. The surgical procedure ensured that the bone grafts remain in place during the period of the experiment.

Bone regeneration due to bioactive phosphate glass is due to the effect of its degradation products. It is known that the dissolution products of bioactive glasses signal the cells (29) and thereby stimulate osteogenesis (8). XG was evaluated as a positive control because it is commercially available, similar in porosity as compared to PPG (approximately 60%) (30), and bioresorbable (31). Histologically the porosity could not be observed in the sections of XG particles (Fig. 5b, 5d) in the rabbit femur model.

On the contrary, the bone regeneration could be observed around and inside the pores of PPG (Fig. 5a, 5c) indicating its porous nature as well as its bioresorption leading to bone regeneration at the early stage of healing. This is a very clear indicator of osteoconductivity of PPG. In the Beagle dog mandible model, PPG particles could be observed in only one histological section (Fig. 6a). In this image, the newly generated bone can be seen in the pores of this PPG particle. This observation supports the SEM (Fig. 3) and micro-CT (Fig. 4) results that the pores of PPG are interconnected and are suitable for mass transport required for bone regeneration. On the contrary, XG particles were completely degraded and a void could be observed at the position of the particles (Fig. 6b). The rounding of these void shapes indicate that the bone regeneration and XG degradation is not a simultaneous phenomenon for XG (32).

Many of the existing studies in literature have compared xenografts with non-porous bioactive glasses (33, 34). As observed from the histomorphometry results in the Beagle dog mandibles (Fig. 7), the bone regeneration potential of PPG and XG is similar. But the SD for PPG is much smaller than the SD observed for XG. The SD is the indicator of predictability of the treatment. Therefore, it can be concluded that PPG has similar bone regeneration potential to XG but better predictability in terms of bone regeneration. In a study by Stavropoulos et al. which compared a bovine bone (a xenograft) and bioactive glass, mean volume of newly formed bone was only 23% and 12.6% respectively (33). Another study reported a similar result: 35.5% vs 25.1% for a XG and a bioactive glass respectively (34). On the contrary, we saw comparable bone fills (bone area %) for XG and PPG (70.76 $\pm$ 4.90 vs 74.14 $\pm$ 9.71 respectively). Attention must be drawn to the fact that PPG is a bioactive glass which is porous, as opposed to the bioactive glass materials (33, 34), and may have resulted in a positive impact on bone regeneration and the overall healing process.

Composites of synthetic bone graft substitutes and biomolecules as well as other cellular mixtures improve their osteoinductive properties (35). Bone graft substitutes with tunable internal porous structure and resorption properties as PPG can be an added advantage if used in aforementioned composite grafts. Work is underway for making stable foam like structures with various internal structures. With realization of such tunability of PPG in terms of its internal structure, the composites can be used for all type of bone structures. Also, further animal studies are required to determine the bone regeneration at the earlier stages of healing to understand the better bone regeneration predictability of PPG in the Beagle dog model after 6 months of healing.

## CONCLUSIONS

The bone regeneration evaluation model of rabbit femur can be used for histological evaluation of particulate bone graft substitutes, though ensuring the presence of the graft at required location during the period of experiment is difficult. Previous studies comparing both materials have reported superior results with xenografts rather than dense and non-porous bioactive glasses. However, as evidenced by results from this study, the porous structure of PPG and a biocompatible composition substantially increases the bone regeneration potential of PPG. The results from the present study demonstrate that PPG promotes osteoconductivity and predictable bone regeneration as compared to commercially available and commonly used xenografts.

## Acknowledgments

The authors would like to thank Hema Chougule and Dr. Supriya Kheur of Regenerative Medicine Laboratory, DY Patil Dental College and Hospital, DY Patil Vidyapeeth, Pune; Dr. Geetanjali Joshi and Jay Dave of the Institute of Bioinformatics and Biotechnology, Savitribai Phule Pune University; and Nitin Dhavale, Neeti Jalnapurkar and Dr. Awanti Golwilkar of AG Diagnostics Pvt. Ltd., Pune for their indispensable technical assistance for the processing of histological samples. The assistance provided by Arun Torris of National Chemical Laboratories for micro CT evaluation is also gratefully acknowledged. The authors would finally like to thank the various staff members at Entrepreneurship Development Center, Pune, for their continuous support for our research work through provision of relevant infrastructure and technical assistance.

## Sources of funding

This work was substantially supported by a Small Business Innovation Research Initiative (SBIRI) grant from the Biotechnology Industrial Research Assistance Council

(BIRAC) of Government of India for the project titled "Preclinical Validation of Alloplasts Made from Bioactive Phosphate Glasses" (Ref. No. BT/SBIRI1006/40/17-SBIRI). The funding body had no role in study design, data collection and analysis, decision to publish, or preparation of the manuscript.

## Conflict of interest

The authors declare no conflicts of interest.

## REFERENCES

1. Acocella A, Bertolai R, Ellis E, Nissan J, Sacco R. Maxillary alveolar ridge reconstruction with monocortical fresh-frozen bone blocks: a clinical, histological and histomorphometric study. J Craniomaxillofac Surg 2012;40(6):525-533.
2. Banwart JC, Asher MA, Hassanein RS. Iliac crest bone graft harvest donor site morbidity. A statistical evaluation. Spine 1995;20(9):1055-1060.
3. Ross LT, JB Miles, N. Heterotopic bone formation causing recurrent donor site pain following iliac crest bone harvesting. Br J Neurosurg 2000;14(5):476-479.
4. Miron RJ, Sculean A, Shuang Y, Bosshardt DD, Gruber R, Buser D, Chandad F, Zhang Y. Osteoinductive potential of a novel biphasic calcium phosphate bone graft in comparison with autographs, xenografts, and DFDBA. Clin Oral Implants Res 2016;27(6):668-675.
5. Sarkar SK, Lee BT. Hard tissue regeneration using bone substitutes: an update on innovations in materials. Korean J Intern Med 2015;30(3):279.
6. Moussa NT, Dym H. Maxillofacial bone grafting materials. Dent Clin North Am 2020;64(2):473-490.
7. Jones JR, Hench LL. Regeneration of trabecular bone using porous ceramics. Curr Opin Solid State Mater Sci 2003;7(4-5):301-307.
8. Hench LL. The story of Bioglass®. J Mater Sci Mater Med 2006;17(11):967-978.
9. Ahmed I, Lewis M, Olsen I, Knowles J. Phosphate glasses for tissue engineering: Part 1. Processing and characterisation of a ternary-based P2O5–CaO–Na2O glass system. Biomaterials 2004;25(3):491-499.
10. Ahmed I, Lewis M, Olsen I, Knowles J. Phosphate glasses for tissue engineering: part 2. Processing and characterisation of a ternary-based P2O5–CaO–Na2O glass fibre system. Biomaterials 2004;25(3):501-507.
11. Xynos ID, Edgar AJ, Buttery LD, Hench LL, Polak JM. Ionic products of bioactive glass dissolution increase proliferation of human osteoblasts and induce insulin-like growth factor II mRNA expression and protein synthesis. Biochem Biophys Res Commun 2000;276(2):461-465.
12. Filho OP, La Torre GP, Hench LL. Effect of crystallization on apatite-layer formation of bioactive glass 45S5. J Biomed Mater Res 1996;30(4):509-514.
13. Bunker B, Arnold G, Wilder JA. Phosphate glass dissolution in aqueous solutions. J Non Cryst Solids 1984;64(3):291-316.
14. Neel EAA, Pickup DM, Valappil SP, Newport RJ, Knowles JC. Bioactive functional materials: a perspective on phosphate-based glasses. J Mater Chem 2009;19(6):690-701.
15. Kiani A, Lakhkar NJ, Salih V, Smith ME, Hanna JV, Newport RJ, Pickup DM, Knowles JC. Titanium-containing bioactive phosphate glasses. Philos Trans A Math Phys Eng Sci 2012;370(1963):1352-1375.
16. Wu ZY, Hill RG, Yue S, Nightingale D, Lee PD, Jones JR. Melt-derived bioactive glass scaffolds produced by a gel-cast foaming technique. Acta Biomater 2011;7(4):1807-1816.
17. Chauhan N, Lakhkar N, Chaudhari A. Development and physicochemical characterization of novel porous phosphate glass bone graft substitute and in vitro comparison with xenograft. J Mater Sci Mater Med 2021;32(6):1-13.
18. Lakhkar NJ, Park J-H, Mordan NJ, Salih V, Wall IB, Kim H-W, King SP, Hanna JV, Martin RA, Addison O. Titanium phosphate glass microspheres for bone tissue engineering. Acta Biomater 2012;8(11):4181-4190.
19. Schindelin J, Arganda-Carreras I, Frise E, Kaynig V, Longair M, Pietzsch T, Preibisch S, Rueden C, Saalfeld S, Schmid B. Fiji: an open-source platform for biological-image analysis. Nat Methods 2012;9(7):676-682.
20. Doube M, Kłosowski MM, Arganda-Carreras I, Cordelières FP, Dougherty RP, Jackson JS, Schmid B, Hutchinson JR, Shefelbine SJ. BoneJ: free and extensible bone image analysis in ImageJ. Bone 2010;47(6):1076-1079.
21. Campion C, Hing KA. Porous Bone Graft Substitutes. When Less is More. In: Rawlinson SCF, editor. Mechanobiology: Exploitation for Medical Benefit. Hoboken, New Jersey: John Wiley & Sons; 2017. p. 347-371.
22. Xynos ID, Edgar AJ, Buttery LD, Hench LL, Polak JM. Gene-expression profiling of human osteoblasts following treatment with the ionic products of Bioglass® 45S5 dissolution. J Biomed Mater Res 2001;55(2):151-157.
23. Hing KA. Bioceramic bone graft substitutes: influence of porosity and chemistry. Int J Appl Ceram Technol 2005;2(3):184-199.
24. Will J, Melcher R, Treul C, Travitzky N, Kneser U, Polykandriotis E, Horch R, Greil P. Porous ceramic bone scaffolds for vascularized bone tissue regeneration. J Mater Sci Mater Med 2008;19(8):2781-2790.
25. Kawamura H, Ito A, Miyakawa S, Layrolle P, Ojima K, Ichinose N, Tateishi T. Stimulatory effect of zinc-releasing calcium phosphate implant on bone formation in rabbit femora. J Biomed Mater Res 2000;50(2):184-190.
26. Fujishiro Y, Hench L, Oonishi H. Quantitative rates of in vivo bone generation for Bioglass® and hydroxyapatite particles as bone graft substitute. J Mater Sci Mater Med 1997;8(11):649-652.
27. Walsh WR, Vizesi F, Michael D, Auld J, Langdown A, Oliver R, Yu Y, Irie H, Bruce W. β-TCP bone graft substitutes in a bilateral rabbit tibial defect model. Biomaterials 2008;29(3):266-271.
28. Aslan M, Şimşek G, Dayi E. The effect of hyaluronic acid-supplemented bone graft in bone healing: experimental study in rabbits. J Biomater Appl 2006;20(3):209-220.
29. Navarro M, Ginebra MP, Planell JA. Cellular response to calcium phosphate glasses with controlled solubility. J Biomed Mater Res A 2003;67(3):1009-1015.
30. Lee JH, Yi GS, Lee JW, Kim DJ. Physicochemical characterization of porcine bone-derived grafting material and comparison with bovine xenografts for dental applications. J Periodontal Implant Sci 2017;47(6):388-401.
31. Thaller SR, Hoyt J, Dart A, Borjeson K, Tesluk H. Repair of experimental calvarial defects with Bio-Oss particles and collagen sponges in a rabbit model. J Craniofac Surg 1994;5(4):242-246.
32. Pinholt EM, Bang G, Haanaes HR. Alveolar ridge augmentation in rats by Bio-Oss. Eur J Oral Sci 1991;99(2):154-161.
33. Stavropoulos A, Kostopoulos L, Nyengaard JR, Karring T. Deproteinized bovine bone (Bio-Oss®) and bioactive glass (Biogran®) arrest bone formation when used as an adjunct to guided tissue regeneration (GTR) An experimental study in the rat. J Clin Periodontol 2003;30(7):636-643.
34. Bassi APF, de Carvalho PSP. Repair of bone cavities in dog's mandible filled with inorganic bovine bone and bioactive glass associated with platelet rich plasma. Braz Dent J 2011;22(1):14-20.
35. Erbe E, Marx J, Clineff T, Bellincampi L. Potential of an ultraporous β-tricalcium phosphate synthetic cancellous bone void filler and bone marrow aspirate composite graft. Eur Spine J 2001;10(2):S141-S146.